



# CHORUS

This is the accepted manuscript made available via CHORUS. The article has been published as:

## Single layer MoS<sub>2</sub> on the Cu(111) surface: First-principles electronic structure calculations

Duy Le, Dezheng Sun, Wenhao Lu, Ludwig Bartels, and Talat S. Rahman

Phys. Rev. B **85**, 075429 — Published 23 February 2012

DOI: [10.1103/PhysRevB.85.075429](https://doi.org/10.1103/PhysRevB.85.075429)

# A single layer MoS<sub>2</sub> on the Cu(111) surface

Duy Le,<sup>1</sup> Dezheng Sun,<sup>2</sup> Wenhao Lu,<sup>2</sup> Ludwig Bartels,<sup>2</sup> and Talat S. Rahman<sup>1,\*</sup>

<sup>1</sup>*Department of Physics, University of Central Florida, Orlando, Florida 32816, United States*

<sup>2</sup>*Pierce Hall, University of California-Riverside, Riverside, California 92521, United States*

(Dated: February 10, 2012)

First principles calculations of the geometric and electronic structures of a single layer of molybdenum disulfide (MoS<sub>2</sub>) on Cu(111) utilizing the van der Waals density functional show three energetically equivalent stacking types and a Moiré pattern whose periodicity is in agreement with experimental findings. The layer is found not to be purely physisorbed on the surface, rather there exists a chemical interaction between it and the Cu surface atoms. We also find that the MoS<sub>2</sub> film is not appreciably buckled, while the top Cu layer gets reorganized and vertically disordered. The sizes of Moiré patterns for a single layer of MoS<sub>2</sub> adsorbed on other close packed metal surfaces are also estimated by minimizing the lattice mismatch between the film and the substrate.

PACS numbers: 68.43.Bc, 81.05.Zx, 61.46.-w, 73.22.-f

## I. INTRODUCTION

It is well-known that a simple material like graphene, which used to be a prototype two dimensional dream material for theorists, has recently been at the center of fundamental and technical discussions around applications of ultrathin layered materials to nanotechnology.<sup>1</sup> Thanks to its novel properties, it has already found a key application in high cutoff frequency transistor.<sup>2</sup> Attention has also turned to other layered materials such as transition-metal dichalcogenides,<sup>3</sup> a prototype of which is molybdenum disulfide (MoS<sub>2</sub>): a single layer of MoS<sub>2</sub> consists of a molybdenum layer sandwiched between two sulfur layers. The recent finding of the transition of MoS<sub>2</sub> from an indirect band gap (of 1.2 eV) bulk material or to a direct band gap ( $\sim 1.8 - 1.9$  eV) in the limit of a single layer<sup>4,5</sup> makes it a promising new material for industrial applications.<sup>6-8</sup> This finding has sparked further interest in seeking ways to grow extended layers of MoS<sub>2</sub>. Very recently, relatively large single layer patches of MoS<sub>2</sub> were grown on Cu(111),<sup>9</sup> displaying a Moiré pattern, whose periodicity is about 1.3 nm, corresponding to  $(5 \times 5)$  Cu(111) surface supercell.

In general, the inhomogeneity in the Moiré pattern suggests a spatial variation of interactions leading to rearrangement of the atoms in the top few layers, as found for graphene<sup>10,11</sup> and hexagonal Boron Nitride<sup>12</sup> on metal surfaces. Furthermore, the extent of the buckling is taken to be a quick measure of the interaction of the overlayer atoms with the substrate: small buckling is typically assumed to signify physisorption. What then is the nature of the binding of MoS<sub>2</sub> layer to the Cu(111) surface? To our knowledge this question is yet to be answered. In addition, we would like to examine: 1) the size of the Moiré pattern for MoS<sub>2</sub> on Cu(111) and how it compares with that on other close packed metal surfaces, 2) how the MoS<sub>2</sub> layer stacks on the Cu(111) surface and whether fingerprints from such stacking may be revealed in Scanning Tunneling Microscopy (STM) images, and 3) the extent to which the interaction results in rearrangement of the adlayer or the substrate.

## II. COMPUTATIONAL DETAILS

We performed first principles electronic structure calculations to evaluate the total energy and electronic structure of the MoS<sub>2</sub> layer on Cu(111) employing the van der Waals density functional (vdW-DF)<sup>13,14</sup> and the efficient algorithm proposed by Román-Pérez and Soler<sup>15</sup> together with the ultra soft pseudo potential method, which are implemented in the Quantum ESPRESSO package.<sup>16</sup> In the spirit of the vdW-DF method, the exchange-correlation energy of the system contains three terms: the exchange energy  $E_x^{GGA}$  from the revised generalized-gradient approximation (GGA) in the form of the Perdew-Burke-Ernzerhof functional (revPBE),<sup>17</sup> the correlation energy  $E_c^{LDA}$  calculated using the local density approximation (LDA), and the nonlocal correlation energy  $E_c^{nl}$ . Our model system consists of a MoS<sub>2</sub> layer on a five-layer Cu(111) slab on top of which we have 15 Å of vacuum. We consider three types of surface super structures:  $(3 \times 3)$  MoS<sub>2</sub> on  $(4 \times 4)$  Cu(111),  $(4 \times 4)$  MoS<sub>2</sub> on  $(5 \times 5)$  Cu(111), and  $(5 \times 5)$  MoS<sub>2</sub> on  $(6 \times 6)$  Cu(111). To obtain the equilibrium configuration for a given structure, as we bring the MoS<sub>2</sub> layer close to the Cu(111) surface in small increments, a minimum in energy is found around 2.6 Å. At this height, we initially arrange the MoS<sub>2</sub> layer such that one S atom sits on a high symmetry substrate site. We then allow all atoms in the system, except for those in the bottom two Cu layers, to undergo ionic relaxation to yield the lowest energy configuration. The two types of hollow sites (fcc and hcp) and the top site<sup>18</sup> lead effectively to three possible stacking of the MoS<sub>2</sub> layer on Cu(111), as we shall see. The Brillouin zone is sampled with a  $(5 \times 5 \times 1)$ ,  $(3 \times 3 \times 1)$ , and  $(1 \times 1 \times 1)$   $\Gamma$ -centered meshes for the  $(4 \times 4)$ ,  $(5 \times 5)$ , and  $(6 \times 6)$  Cu(111) substrate supercells, respectively. We set the cutoff energy for the plane wave expansion to 35 Ry and for the augmentation charge to 420 Ry. All structures are relaxed until all force components acting on each atom reach the 0.01 eV/Å threshold. We find the lattice parameters of bulk Cu and of the MoS<sub>2</sub> layer, estimated by the vdW-DF approximation, to be 3.690

Å and 3.255 Å, respectively, which are about 2 – 3% higher than experimental values for Cu (3.61 Å)<sup>19</sup> and MoS<sub>2</sub> (3.16 Å).<sup>20</sup>

We calculate the average binding energy  $E_b$  per MoS<sub>2</sub> unit according to:

$$E_b = \frac{1}{n_1^2} [E_{\text{MoS}_2/\text{Cu}(111)} - E_{\text{Cu}(111)} - E_{\text{MoS}_2}]; \quad (1)$$

where  $E_{\text{MoS}_2/\text{Cu}(111)}$ ,  $E_{\text{Cu}(111)}$  and  $E_{\text{MoS}_2}$  are the total energy of, respectively, the  $(n_1 \times n_1)$  MoS<sub>2</sub> on  $(n_2 \times n_2)$  Cu(111) system, clean  $(n_2 \times n_2)$  Cu(111) slab, and  $(n_1 \times n_1)$  free standing MoS<sub>2</sub> film.

### III. RESULTS AND DISCUSSIONS

#### A. Moiré pattern periodicity

As is known, Moiré pattern results from the mismatch between the intrinsic periodicity of the overlayer and the substrate. This mismatch for an  $(n_1 \times n_1)$  super-structure on  $(n_2 \times n_2)$  close packed metal (M) substrate unit, may be defined conveniently by a parameter:

$$m = \frac{n_1 d_S}{n_2 d_M} - 1; \quad (2)$$

where  $d_S$  is the lattice parameter of the overlayer and  $d_M$  is  $a_M/\sqrt{2}$  for fcc metal, and  $a_M$  for hcp metals, where  $a_M$  is the metal lattice parameter. From geometric consideration, the smaller the value of this parameter, the smaller would be the stress in the surface. For Cu(111), the experimental lattice parameters yield  $d_{\text{Cu}}$  at about 2.255 Å and  $d_S$  for MoS<sub>2</sub> is around 3.16 Å. If we limit  $n_2$  to 20, we find the  $(4 \times 4)$  overlayer on a  $(5 \times 5)$  substrate supercell to have the lowest absolute value of  $m$  (-1.0%). This result agrees very well with the size of Moiré unit cell observed in a recent STM experiment.<sup>9</sup> The two nearest-sized supercells to the preferred one,  $(5 \times 5)$  MoS<sub>2</sub> on  $(6 \times 6)$  Cu(111) and  $(3 \times 3)$  MoS<sub>2</sub> on  $(4 \times 4)$  Cu(111), have  $m$  of 3.2% and -7.2%, respectively.

TABLE I. Predicted sizes of MoS<sub>2</sub> Moiré unit cell on several close packed metal surfaces. ( $n_2 \leq 20$ )

Surfaces	$d_M$ (Å) <sup>a</sup>	$n_1$	$n_2$	$m$ (%)
Ag(111)	2.89	10	11	-0.7
Cu(111)	2.55	4	5	-1.0
Ni(111)	2.49	11	14	-0.2
		15	19	0.2
Pt(111)	2.77	7	8	-0.2
Rh(111)	2.69	6	7	0.8
		11	13	-0.5
		17	20	0.0
Ir(111)	2.72	6	7	-0.2
Re(0001)	2.76	7	8	0.2
Ru(0001)	2.71	6	7	-0.1

<sup>a</sup> Calculated from experimental lattice parameters<sup>19</sup>

Interestingly, several other close packed metal surfaces offer an even smaller value of  $m$  for a MoS<sub>2</sub> layer. A summary of our calculated minimum value of  $m$  corresponding to  $(n_1 \times n_1)$  MoS<sub>2</sub> structure over  $(n_2 \times n_2)$  metal unit cell ( $n_2 \leq 20$ ) is presented in Table I.

As further quantification of the Moiré pattern periodicity, we find the calculated average binding energy of the appropriate MoS<sub>2</sub> structure for the  $(4 \times 4)$ ,  $(5 \times 5)$ , or  $(6 \times 6)$  Cu(111) substrate unit cell to be, respectively, -0.03 eV, -0.27 eV, and -0.16 eV. Once again, the average binding energy is lowest for  $(4 \times 4)$  MoS<sub>2</sub> on  $(5 \times 5)$  Cu(111), in agreement with experimental findings.<sup>9</sup>

#### B. Geometry of MoS<sub>2</sub> on Cu(111)

Turning our attention to the most favorable structure, the  $(4 \times 4)$  MoS<sub>2</sub> on  $(5 \times 5)$  Cu(111), we first note that after ionic relaxation, three types of stacking (Fig. 1) are produced. In these, labeled as  $\alpha$ ,  $\beta$ , and  $\gamma$ , the high symmetry center is in registry with, respectively, the fcc hollow, top, and hcp hollow site on Cu(111). Here, the high symmetry center is defined as the center of the smallest up-pointing triangle in Fig. 1 whose vertices are three equivalent S atoms. The average binding energy of the MoS<sub>2</sub> film on Cu(111) is -0.27 eV irrespective of the stacking type. From the centers of the high symmetry regions, one can plot five rings, labeled R1 to R5, with radii 1.86, 3.73, 4.95, 6.78, and 7.54 Å ( $\alpha$  stacking) so that each ring goes through equivalent S atoms. These radii are 1.89, 3.80, 4.99, 6.80, and 7.53 Å for  $\beta$  stacking and 1.90, 3.76, 5.00, 6.79, and 7.53 Å for  $\gamma$  stacking. The number of interfacial S atoms on each ring is, respectively, 3, 3, 6, 6, and 3. The S atoms in R5 are in registry with the hcp, fcc, and top sites in the  $\alpha$ ,  $\beta$ , and  $\gamma$  stacking, respectively. The distance of the S atoms of the lower layer on each ring to their closest Cu atom are, respectively, 2.47, 2.57, 2.70, 2.95, and 3.04 Å in  $\alpha$  stacking, 2.95, 2.57, 2.70, 2.47, and 3.06 Å in  $\beta$  stacking, and 2.82, 2.95, 2.56, 2.81, and 2.46 Å in  $\gamma$  stacking. These distances are larger than the typical S-Cu bond-length (2.22 – 2.29 Å, depending on adsorption sites)<sup>22,23</sup> for Cu(111).

Note that the choice of the center of the high symmetry region is not unique. In fact, in each Moiré pattern unit-cell there is another high-symmetry point (down-pointing triangle in Fig. 1) where a Mo atom is centered over a substrate Cu atom ( $\alpha$ ), hcp hollow ( $\beta$ ) or fcc hollow ( $\gamma$ ). We opted to choose the center of up-pointing triangles because the footprints of the vertices of these triangles can be distinguished easily in the simulated STM images (Fig. 2a and 2b): they are the brightest spots in the  $\alpha$  stacking case, the least bright in the  $\beta$  stacking case, and neither the least bright nor the brightest in the  $\gamma$  stacking. On the other hand, the vertices of down-pointing triangles are displayed as the brightest spots in the  $\beta$  case, less (but not the least) in the  $\alpha$  case, and the least bright in the  $\gamma$  case. Regardless,

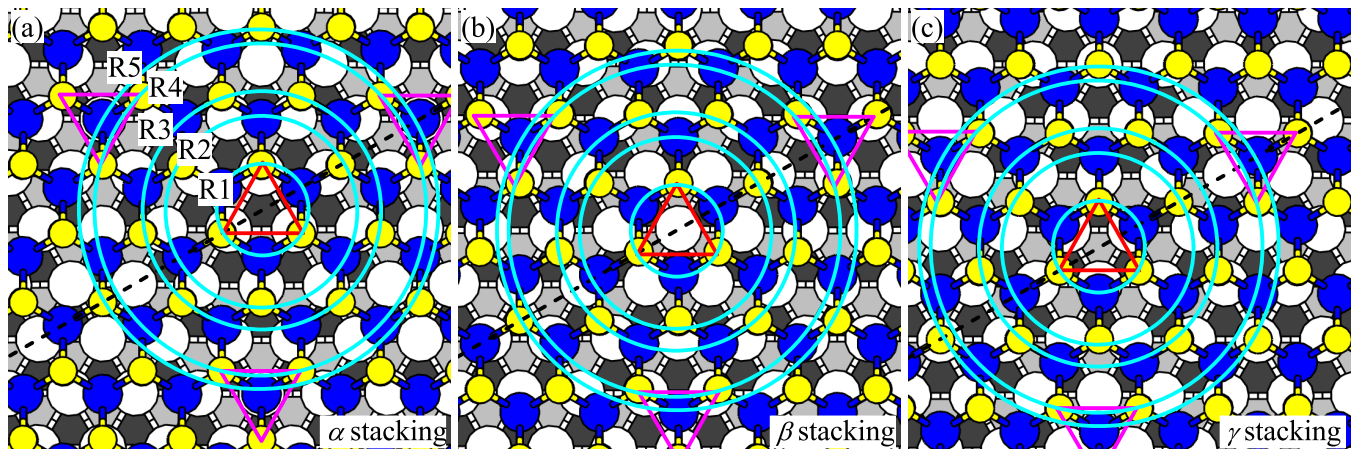


FIG. 1. (Color online) Atomic model of a single layer MoS<sub>2</sub> in  $\alpha$  (a),  $\beta$  (b), and  $\gamma$  (b) stacking on Cu(111). Yellow (gray), blue (dark), and white circles represent S, Mo, Cu surface atoms, respectively. The dark and light gray spaces between Cu surface atoms are, respectively, fcc and hcp sites of the Cu(111) surface. Rings numbered from R1 to R5 highlight the equivalent S atoms. Triangles highlight groups of three equivalent S atoms. Dashed lines indicate the direction of the shifts between stacking types.

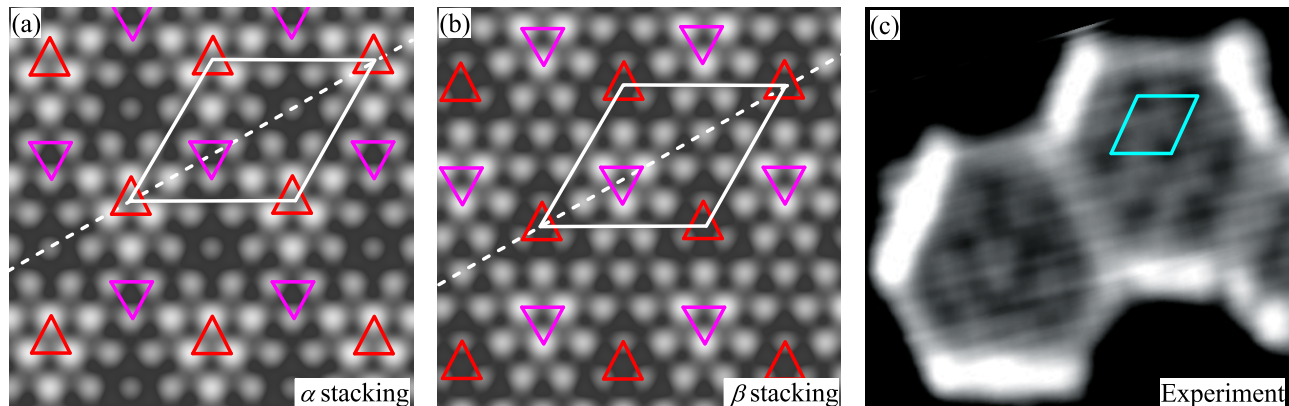


FIG. 2. (Color online) (a) and (b)  $19 \times 19 \text{ \AA}^2$  Simulated STM image<sup>21</sup> of  $\alpha$  and  $\beta$  stacking. The color scale goes from dark to bright corresponding to the height from 0  $\text{\AA}$  to 0.34  $\text{\AA}$ . Bias voltage is  $-0.560 \text{ V}$  and iso LDOS value is  $10^{-6} \text{ Ry}^{-1}$ . A  $7 \times 7 \times 1$  mesh is used to sample the Brillouin zone. Up and down-pointing triangles highlight the three spots with the same contrast and corresponding to those in Fig. 1. Parallelograms indicate the Moiré unitcells. (c) STM image of two adjacent MoS<sub>2</sub> island for comparing the difference in appearance of the Moiré pattern to panels (a) and (b). The parallelogram indicates the Moiré unitcell. The image size is  $11.5 \text{ nm} \times 10.5 \text{ nm}$ , the bias is  $-0.475 \text{ V}$  and the tunneling current is  $110 \text{ pA}$ .

the analysis above provides fingerprints for identifying stacking types from high atomic-resolution STM images of MoS<sub>2</sub>/Cu(111) systems: for images, recorded at voltage of about  $-0.5 \text{ V}$ , if the brightest spots are the vertices of the smallest up-pointing triangles (with respect to the orientation shown in Fig. 1), the stacking is  $\alpha$  type, if they are those of the down-pointing triangle it is  $\beta$  type, otherwise it belongs to  $\gamma$  type.

The existence of different types of registries of MoS<sub>2</sub> layer with Cu(111) is also seen in experimental STM images of MoS<sub>2</sub> flakes on Cu(111). MoS<sub>2</sub> flakes have been grown in UHV (base pressure  $< 2 \times 10^{-10}$ ) by a sequence of deposition of thiophenol onto a sputter-and-anneal cleaned Cu(111) substrate at  $\sim 100 \text{ K}$  and  $10^{-7} \text{ Torr}$  for 300 s, followed by annealing to  $\sim 400 \text{ K}$  to re-

move the phenyl groups. Subsequently, Mo metal is deposited using an e-beam evaporator (Omicron) with ion suppressor, followed by sample is annealing to  $\sim 500 \text{ K}$  for 20 mins, to form MoS<sub>2</sub> flakes in various sizes. Image acquisition proceeded after cool-down to  $80 \text{ K}$ . Further details can be found in Ref. 9. Fig. 2c shows two adjacent MoS<sub>2</sub> islands in the same orientation as in Fig. 1. One threefold degenerate MoS<sub>2</sub> edge appears as protrusions in STM because it contains an extra sulfur atom.<sup>24</sup> Inside the islands, the Moiré pattern is visible and clearly different in appearance as predicted in this study.

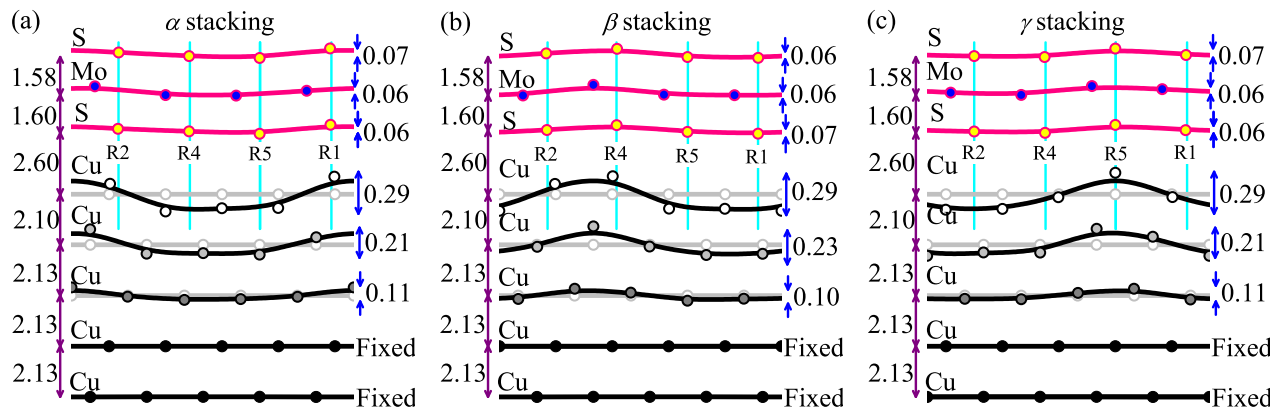


FIG. 3. (Color online) *Intra-layer* buckling along the long diagonal of Moiré unit cells of  $\alpha$  (a),  $\beta$  (b), and  $\gamma$  (c) stacking. Circles represent S, Mo, and Cu atoms. B-spline fits (solid lines) are included for eye guidance purpose. Vertical lines shows point out relative positions of the rings R1, R2, R4, and R5. The numbers (in Å) in the left and right are the average *inter-layer* distances and the buckling of layers.

### C. Interaction between MoS<sub>2</sub> and Cu(111)

The relatively large separation ( $\sim 2.6$  Å) of the bottom S layer and the Cu(111) surface (see Fig. 3) and the low binding energy per MoS<sub>2</sub> unit ( $-0.27$  eV) would at the outset imply a weak interaction, which in turn suggest a small corrugation of the film. Detailed analysis of *intra-layer* buckling – the difference between the  $z$  coordinate of the highest and the lowest atoms of the topmost S layer – at  $\sim 0.06 - 0.07$  Å is much smaller than that known for GR on most substrates.<sup>25</sup> Our calculations also find similar low values for the buckling of the lower S and the Mo layers. Interestingly, the buckling of the top three Cu layers is larger, at  $0.29$  Å,  $0.23$  Å, and  $0.10$  Å, respectively. A similar trend is found for the other two cases, i.e.  $(3 \times 3)$  MoS<sub>2</sub> on  $(4 \times 4)$  Cu(111) and  $(5 \times 5)$  MoS<sub>2</sub> on  $(6 \times 6)$  Cu(111).

There appears to be a correlation between the ripple of the Cu layer and the brightness of the spots in the simulated STM images in Fig. 1. The periodic ripple of the Cu(111) surface leads to the inhomogeneity in interaction between the Cu surface and MoS<sub>2</sub> which is, in turn, represented by the displacement of Cu atoms on the top layer. The more they move up towards the MoS<sub>2</sub> layer, the stronger is the interaction between MoS<sub>2</sub> and the Cu surface. In Fig. 3, one can see the modulation of the Cu surface in the  $\alpha$  stacking is the largest near ring R1, resulting the brightest spots in the simulated STM image, and the smallest near rings R5 and R4 causing less bright spots. Similar effect can also seen for the case of  $\beta$  stacking in which the largest modulation of the Cu surface is near ring R4 corresponding to the brightest spots in its STM image and the least modulation is near ring R1 resulting in the least bright spots. In the case of  $\gamma$  stacking, the largest modulation of Cu(111) is at ring R5 and the smallest modulation is near ring R2 and R4 leading to the brightest and less bright spots in STM image, respectively.

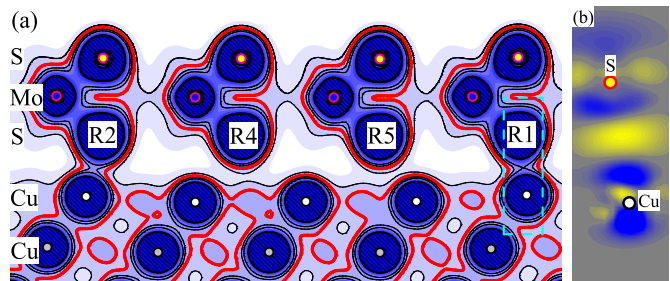


FIG. 4. (Color online) (a) Valence charge density along the vertical plane passing through the long diagonal of the Moiré unit cell of the  $\alpha$  stacking of MoS<sub>2</sub> on Cu(111). R1, R2, R4, and R5 indicate the rings (see Fig. 1a) to which S atoms belong. The labels (S, Mo, Cu) on the left map the rows of S, Mo, and Cu, respectively. Contour values are 0.02, 0.03, 0.04, 0.05, and 0.09 a.u. The 0.03 contour is highlighted (the thickest line) for guidance the eyes.

(b) Density of redistribution of charge in the region limited by a broken rectangular in panel (a). Yellowish (bright) and blueish (dark) regions indicate, respectively, accumulation and depletion of charge. The gray background correspond to zero redistribution. The scale going from blue (dark) to yellow (bright) corresponds to the variation from  $-7.5 \times 10^{-3}$  to  $7.5 \times 10^{-3}$  a.u.

Another indication of the inhomogeneous interaction between the MoS<sub>2</sub> layer and the surface Cu atoms is seen in the plot of the charge density distribution, Fig. 4a ( $\alpha$  stacking as example) which shows an appreciable amount of charge in the region between the S atoms in rings R1 and R2 and their nearest Cu surface atoms but not much in the region near other rings. Calculated charge redistribution upon adsorption of MoS<sub>2</sub> on Cu(111), Fig. 4b, confirms a noticeable accumulation of charge in these regions. This is a signal of chemical bonding – albeit weak – between S in ring R1 and Cu atoms. Similar type of bonding is also form between S in ring R2 and Cu atoms.

#### IV. CONCLUSIONS

In conclusion, our calculated optimum size of the Moiré pattern is in agreement with experimental observations. We have also predicted the size of Moiré patterns for MoS<sub>2</sub> on several close packed metal surfaces by minimizing their mismatch parameters. We show the presence of three energetically equivalent stacking types ( $\alpha$ ,  $\beta$ , and  $\gamma$ ) of MoS<sub>2</sub> on Cu(111) with distinguishable fingerprints in their STM images. Our structural analysis displays very little corrugation of the MoS<sub>2</sub> layer but noticeable rearrangement of the Cu surface atoms. More impor-

tantly, we find the MoS<sub>2</sub> overlayer to be chemisorbed, albeit weakly, to the Cu(111) surface.

#### ACKNOWLEDGMENTS

All simulations in this work were performed using computational resource from STOKES High Performance System at the University of Central Florida. This work was supported in part by U.S. Department of Energy under grant DE-FG02-07ER15842. L.B. was also supported from National Science Foundation under grant NSF DMR-1106210.

- 
- \* Corresponding author: Talat.Rahman@ucf.edu
- <sup>1</sup> A. H. Castro Neto, F. Guinea, N. M. R. Peres, K. S. Novoselov, and A. K. Geim, *Rev. Mod. Phys.* **81**, 109 (2009).
  - <sup>2</sup> Y. Wu, Y. ming Lin, A. A. Bol, K. A. Jenkins, F. Xia, D. B. Farmer, Y. Zhu, and P. Avouris, *Nature* **472**, 74 (2011).
  - <sup>3</sup> A. Ayari, E. Cobas, O. Ogundadegbe, and M. S. Fuhrer, *J. Appl. Phys.* **101**, 014507 (2007).
  - <sup>4</sup> K. F. Mak, C. Lee, J. Hone, J. Shan, and T. F. Heinz, *Phys. Rev. Lett.* **105**, 136805 (2010).
  - <sup>5</sup> A. Splendiani, L. Sun, Y. Zhang, T. Li, J. Kim, C.-Y. Chim, G. Galli, and F. Wang, *Nano Lett.* **10**, 1271 (2010).
  - <sup>6</sup> Y. Yoon, K. Ganapathi, and S. Salahuddin, *Nano Lett.* **11**, 3768 (2011).
  - <sup>7</sup> B. Radisavljevic, A. Radenovi, J. Brivio, V. Giacometti, and A. Kis, *Nature Nanotech.* **6**, 147 (2011).
  - <sup>8</sup> S. Ghatak, A. N. Pal, and A. Ghosh, *ACS Nano* **5**, 7707 (2011).
  - <sup>9</sup> D. Kim, D. Sun, W. Lu, Z. Cheng, Y. Zhu, D. Le, T. S. Rahman, and L. Bartels, *Langmuir* **27**, 11650 (2011).
  - <sup>10</sup> W. Moritz, B. Wang, M.-L. Bocquet, T. Brugger, T. Greber, J. Winterlin, and S. Günther, *Phys. Rev. Lett.* **104**, 136102 (2010).
  - <sup>11</sup> D. Stradi, S. Barja, C. Díaz, M. Garnica, B. Borca, J. J. Hinarejos, D. Sánchez-Portal, M. Alcamí, A. Arnau, A. L. Vázquez de Parga, et al., *Phys. Rev. Lett.* **106**, 186102 (2011).
  - <sup>12</sup> R. Laskowski, P. Blaha, T. Gallauner, and K. Schwarz, *Phys. Rev. Lett.* **98**, 106802 (2007).
  - <sup>13</sup> M. Dion, H. Rydberg, E. Schröder, D. C. Langreth, and B. I. Lundqvist, *Phys. Rev. Lett.* **92**, 246401 (2004).
  - <sup>14</sup> T. Thonhauser, V. R. Cooper, S. Li, A. Puzder, P. Hyldgaard, and D. C. Langreth, *Phys. Rev. B* **76**, 125112 (2007).
  - <sup>15</sup> G. Román-Pérez and J. M. Soler, *Phys. Rev. Lett.* **103**, 096102 (2009).
  - <sup>16</sup> P. Giannozzi, S. Baroni, N. Bonini, M. Calandra, R. Car, C. Cavazzoni, D. Ceresoli, G. L. Chiarotti, M. Cococcioni, I. Dabo, et al., *J. Phys.: Condens. Matter* **21**, 395502 (2009).
  - <sup>17</sup> Y. Zhang and W. Yang, *Phys. Rev. Lett.* **80**, 890 (1998).
  - <sup>18</sup> We also considered an S atom at a bridge site as initial configuration. However, results are identical with ones for S atom at top site.
  - <sup>19</sup> C. Kittel, *Introduction to Solid State Physics* (Wiley, 1995), 7th ed.
  - <sup>20</sup> T. Böker, R. Severin, A. Müller, C. Janowitz, R. Manzke, D. Voß, P. Krüger, A. Mazur, and J. Pollmann, *Phys. Rev. B* **64**, 235305 (2001).
  - <sup>21</sup> J. Tersoff and D. R. Hamann, *Phys. Rev. Lett.* **50**, 1998 (1983); *Phys. Rev. B* **31**, 805 (1985).
  - <sup>22</sup> X.-Y. Pang, L.-Q. Xue, and G.-C. Wang, *Langmuir* **23**, 4910 (2007).
  - <sup>23</sup> M. May, S. Gonzalez, and F. Illas, *Surf. Sci.* **602**, 906 (2008).
  - <sup>24</sup> M. V. Bollinger, J. V. Lauritsen, K. W. Jacobsen, J. K. Nørskov, S. Helveg, and F. Besenbacher, *Phys. Rev. Lett.* **87**, 196803 (2001).
  - <sup>25</sup> C. Busse, P. Lazić, R. Djemour, J. Coraux, T. Gerber, N. Atodiressei, V. Caciuc, R. Brako, A. T. N'Diaye, S. Blügel, et al., *Phys. Rev. Lett.* **107**, 036101 (2011).